

SUPPLEMENTARY INFORMATION

Shining Light on an mGlu5 Photoswitchable NAM: A Theoretical Perspective

Giraldo Jesus*

Laboratory of Molecular Neuropharmacology and Bioinformatics, Institut de Neurociències and Unitat de Bioestadística, Universitat Autònoma de Barcelona, 08193 Bellaterra, Spain

SI Table 1. Potency of Quisqualate, MPEP and alloswitch-1 on rat mGlu5 WT and Q646A or P654M rat mGlu5 mutant receptors (mutations are equivalent to Q647A and P655M in human mGlu5).

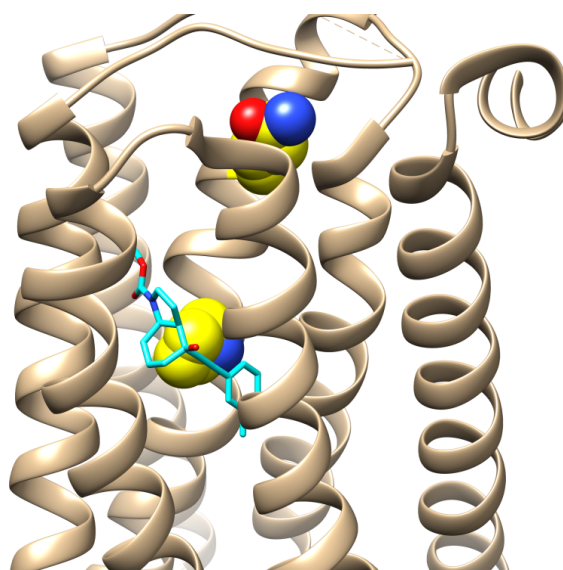
	Quis EC50 (nM) ± SEM (n)	MPEP EC50 (nM) ± SEM (n)	Alloswitch-1 EC50 (nM) ± SEM (n)
WT	7,35 ± 0,25 (3)	7,67 ± 0,09 (3)	7,68 ± 0,15 (3)
Q646A	7,63 ± 0,21 (3)	7,25 ± 0,07 (3)	7,43 ± 0,02 (3)
P654M	7,50 ± 0,29 (3)	ND (3)	ND (3)

SI Table 2. Autodock-4.2 docking scores of top-ranked solutions (expressed as predicted Ki, nM) for MPEP, mavoglurant and four different conformations of alloswitch-1 in mGlu5.

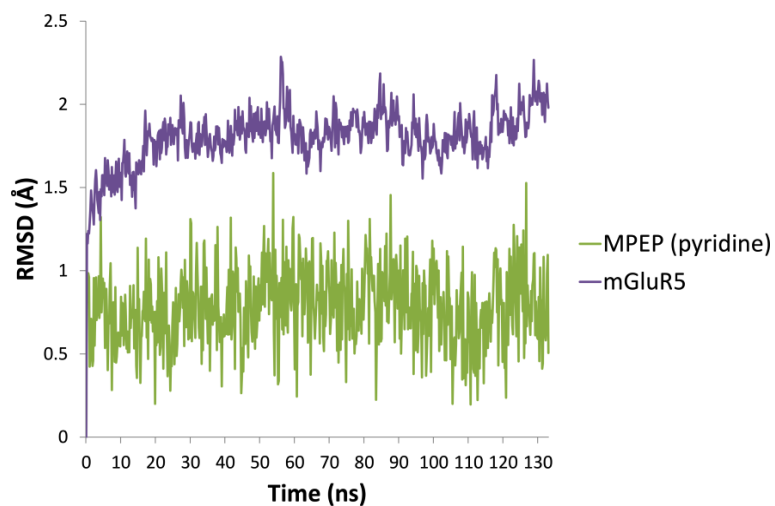
	Alloswitch-1, <i>cis</i> -Amide (in <i>wt</i> mGlu5)	Alloswitch-1, <i>trans</i> -Amide (in <i>wt</i> mGlu5)	Alloswitch-1, <i>trans</i> -amide (in Alternative mGlu5 Conformation)	Alloswitch-1 Photoisomer, <i>cis</i> -azo, in <i>wt</i> mGlu5)	MPEP (in <i>wt</i> mGlu5)	Mavoglurant (in <i>wt</i> mGlu5)
Docking score (Ki, nM)	31.5	697.4	95.0	214.4	430.0	2.8

SI Table 3. Output of NAMDenegy calculations for three different MD simulations of mGlu5 with three different docked conformations of alloswitch-1.

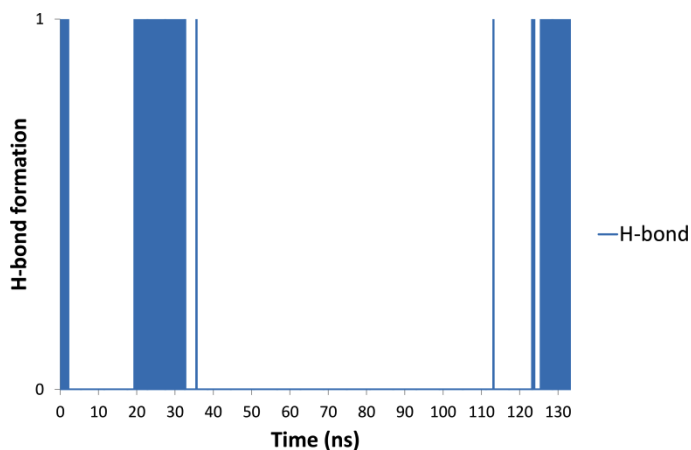
Average Potential Energy (over 100 ns MD, kcal/mol)	Alloswitch-1, <i>cis</i> -amide	Alloswitch-1, <i>trans</i> -amide	Photoswitched Alloswitch-1, <i>trans</i> -amide, <i>cis</i> -azo
Ligand (internal bonded and non-bonded terms)	88.4	84.9	91.7
Protein-ligand (non-bonded terms)	-63.6	-60.0	-61.6



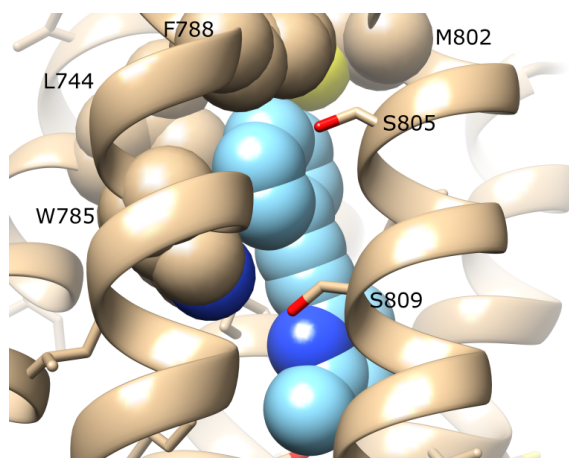
SI Fig. (1). Position of two chosen mutation sites (in yellow) in the allosteric pocket of mGlu5 (in beige) relative to mavoglurant (in cyan, PDB id: 4OO9). Mutation of Q647 (top) and P655 (bottom) are designed to characterize NAM binding in the top and bottom of the allosteric pocket, respectively.



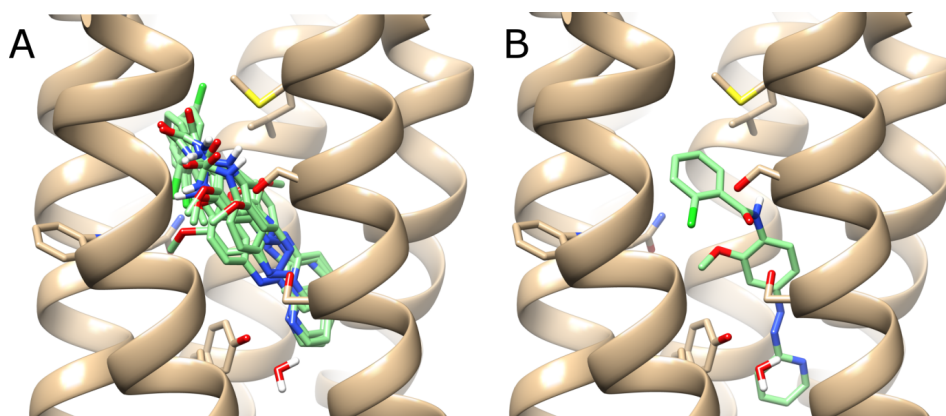
SI Fig. (2). Plot of RMSD (Å) during an MD simulation of mGlu5 with MPEP.



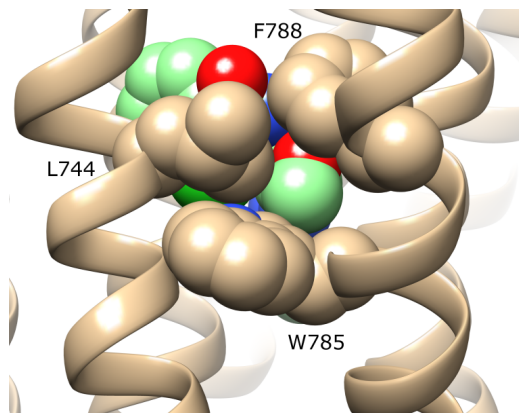
SI Fig. (3). A plot of H-bond formation between S809 and MPEP during an MD simulation of mGlu5.



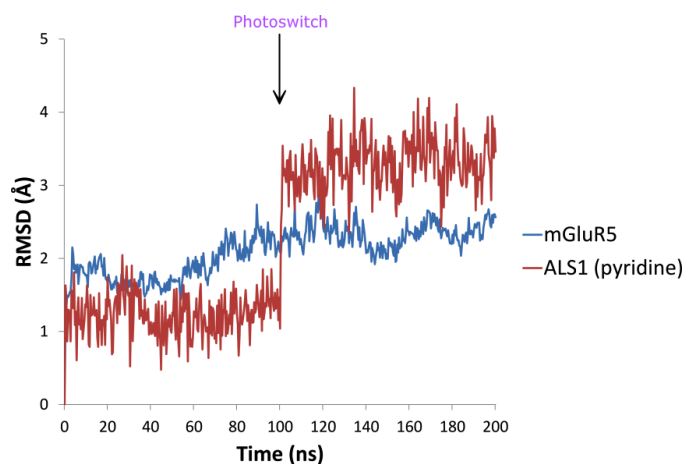
SI Fig. (4). During an MD simulation, planar adjustment of MPEP (in blue) increases hydrophobic interactions with L744 (TM5), W785, F788 (TM6) and M802 (TM7) in the complete *wt* structure of mGlu5 (in beige). TM6 is foreground left and TM7 is foreground right. In the background, TM5 is far left, TM3 is central and TM2 is far right.



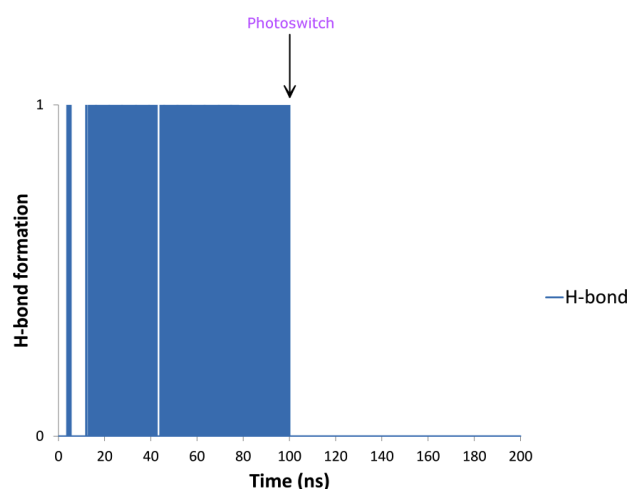
SI Fig. (5). **A**) The 7 best-ranked docking solutions (out of 10) of the active isomer of alloswitch-1 (in green) in the complete *wt* structure of mGlu5 (in beige) where the ligand adopts a *cis*-amide conformation. All ligand *cis*-amide conformations closely overlap with a maximum RMSD between conformers: 2.9 Å, and predicted K_i docking scores in the range of 31-388 nM. **B**) The 10th (and lowest-ranked) docking solution of alloswitch-1 where the ligand adopts a *trans*-amide conformation (in green) in *wt* structure of mGlu5 (beige), with predicted K_i docking score of 697 nM. In this docking, alloswitch-1 clashes with the co-crystallized water molecule and Y659 at the bottom of the allosteric pocket. In both (A) and (B), TM6 is foreground left and TM7 is foreground right. In the background, TM5 is far left, TM3 is central and TM2 is far right.



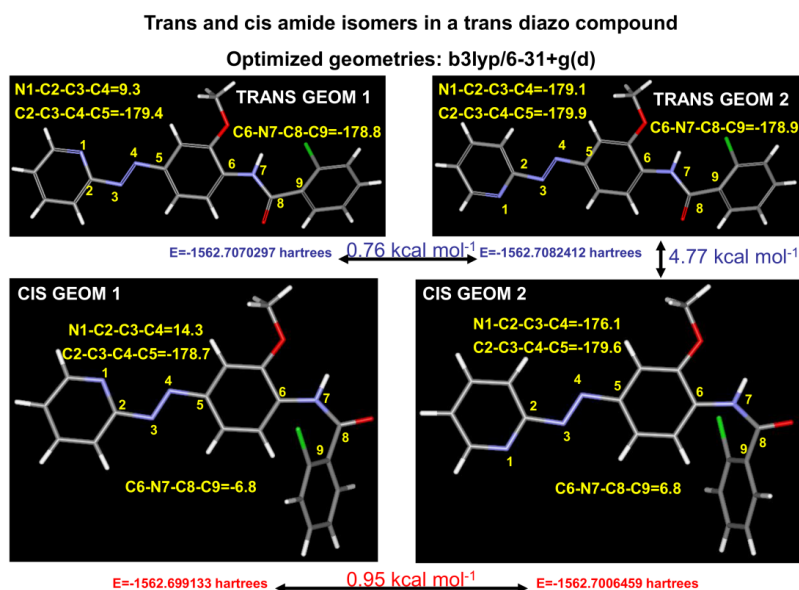
SI Fig. (6). Alloswitch-1 with a *cis*-amide (in green) bound to *wt* mGlu5 (beige) after 100 ns of MD simulation “in the dark” (beginning from top-ranked docking solution of alloswitch-1 in the *wt* crystal structure of mGlu5). The methoxy group of alloswitch-1 binds between three residues on TM5 (L744) and TM6 (W785, F788), partially moving out of plane of the ligand.



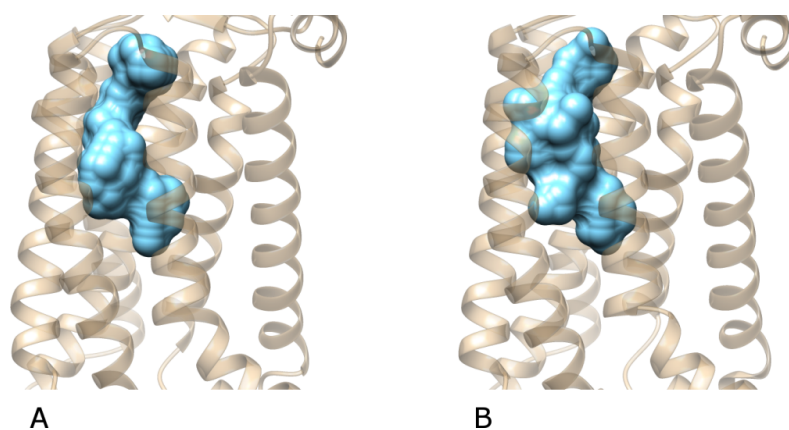
SI Fig. (7). Plot of RMSD (Å) during an MD simulation of mGlu5 with alloswitch-1 in a *cis*-amide conformation. After 100 ns, a photoswitch of alloswitch-1 is simulated by adjusting the azo group into a *cis*-state (*trans*-state in normal conditions).



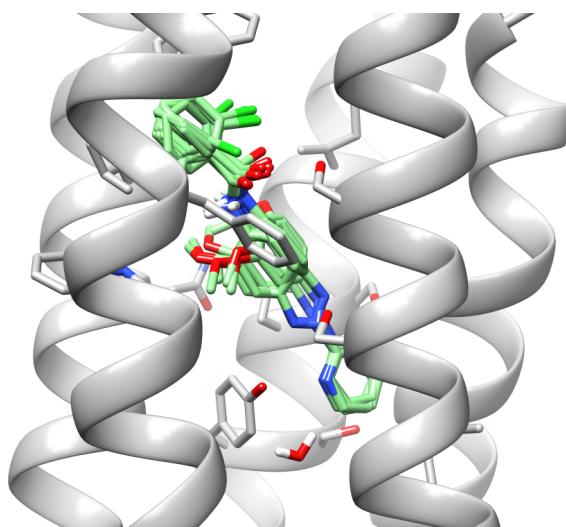
SI Fig. (8). A plot of H-bond formation between S809 and alloswitch-1 in a *cis*-amide conformation during an MD simulation of mGlu5. After 100 ns, a photoswitch of alloswitch-1 is simulated by adjusting the azo group into a *cis*-state (*trans*-state in normal conditions).



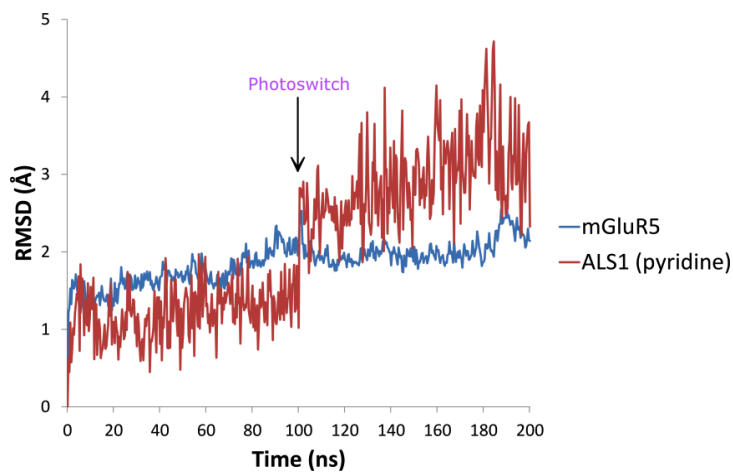
SI Fig. (9). Optimization of *cis*-amide and *trans*-amide conformations of alloswitch-1 with Density Functional Theory (DFT) at the B3LYP/6-31+G(d) level.



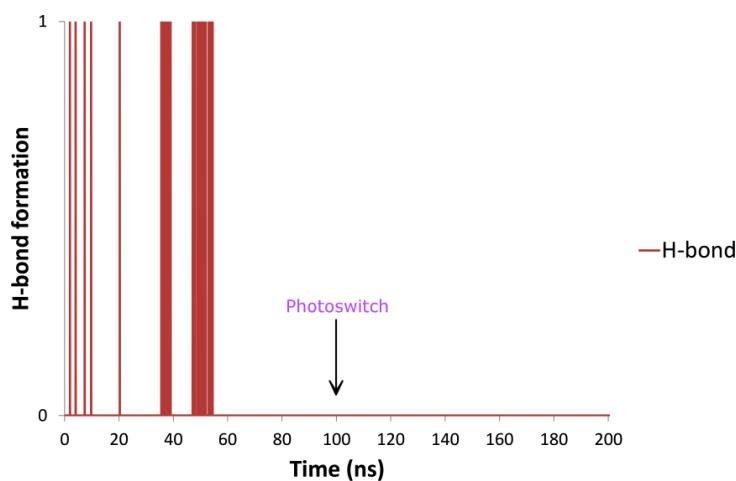
SI Fig. (10). Two alternative conformations of mGlu5: (A) the original crystal structure (PDB id: 4OO9) and (B) an alternative state with a wider allosteric pocket identified by ROSETTA relaxation. The protein is coloured beige and the volume of the allosteric pocket is coloured blue.



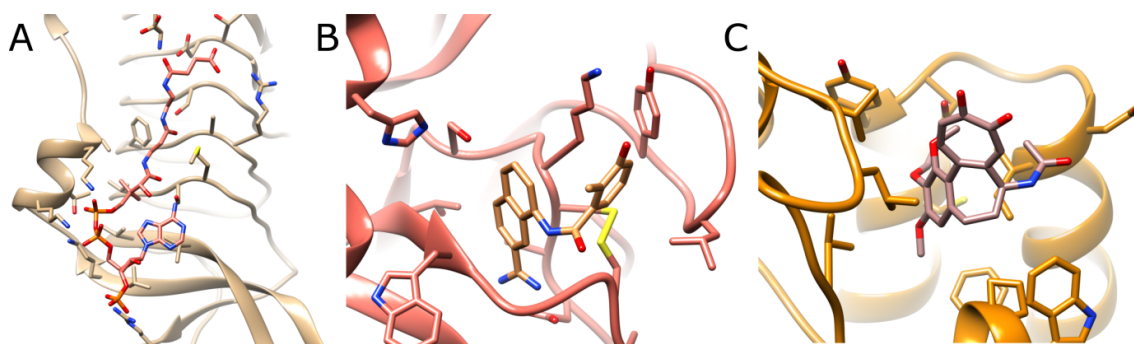
SI Fig. (11). All 10 alternative docking solutions of the active isomer of alloswitch-1 (in green) in an alternative receptor conformation of mGlu5 (in grey) where the ligand adopts a *trans*-amide conformation. All ligand *trans*-amide conformations closely overlap with a maximum RMSD between conformers: 2.3 Å, and predicted K_i docking scores in the range of 95-315 nM. TM6 is foreground left and TM7 is foreground right. In the background, TM5 is far left, TM3 is central and TM2 is far right.



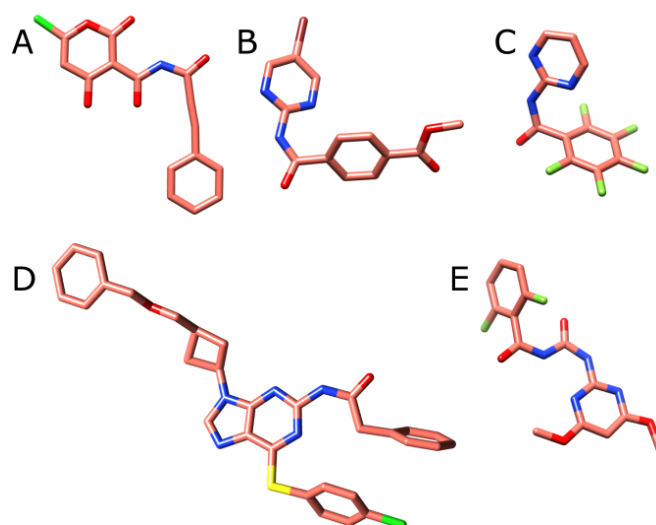
SI Fig. (12). Plot of RMSD (Å) during an MD simulation of an alternative conformation of mGlu5 with alloswitch-1 in a *trans*-amide conformation. After 100 ns, a photoswitch of alloswitch-1 is simulated by adjusting the azo group into a *cis*-state (*trans*-state in normal conditions).



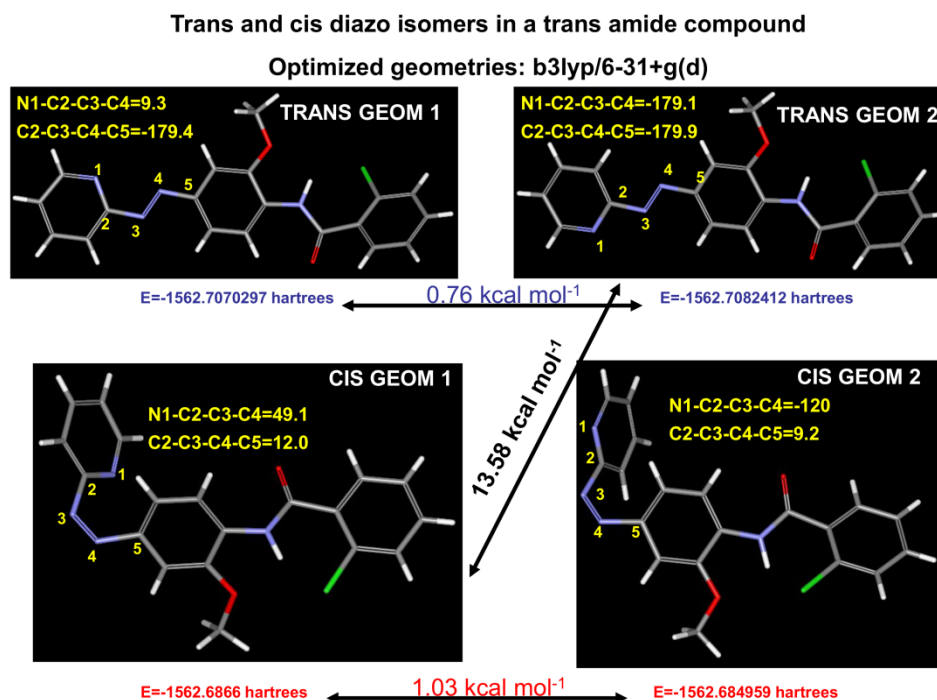
SI Fig. (13). A plot of H-bond formation between S809 and alloswitch-1 in a *trans*-amide conformation during an MD simulation of an alternative conformation of mGlu5. After 100 ns, a photoswitch of alloswitch-1 is simulated by adjusting the azo group into a *cis*-state (*trans*-state in normal conditions).



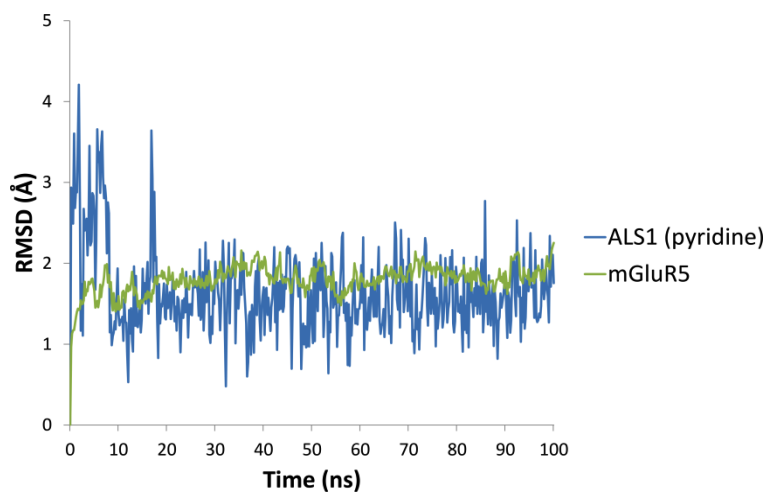
SI Fig. (14). Selected *cis*-amide ligand-protein complexes in the PDB: (A) Tetrahydrodipicolinate N-Succinyltransferase in complex with Succinamide-CoA (PDB id: 1KGQ), (B) Coagulation Factor XI in complex with N-(7-Carbamimidoyl-naphthalen-1-yl)-3-hydroxy-2-methylbenzamide (PDB id: 1ZSJ), (C) Bromodomain-containing protein 4 in complex with Colchicine (PDB id: 4LYS).



SI Fig. (15). Selected *cis*-amide small-molecule compounds identified in the CSD: (A) 6-chloro-4-hydroxy-2-oxo-N-(3-phenylprop-2-ynoyl)-2H-pyran-3-carboxamide, (B) Methyl 4-[N-(5-bromopyrimidin-2-yl)-carbamoyl]benzoate, (C) N-(Pyrimidin-2-yl)pentafluorobenzamide, (D) 9-(cis-3-(Benzyloxymethyl)cyclobutyl)-6-(4-chlorophenylsulfanyl)-2-(phenylacetamido)-9H-purine, (E) N-(2,6-Difluorobenzoyl)-N'-(4,6-dimethoxypyrimidin-2-yl)urea.



SI Fig. (16). Optimization of *cis*-azo and *trans*-azo conformations of alloswitch-1 with Density Functional Theory (DFT) at the B3LYP/6-31+G(d) level.



SI Fig. (17). Plot of RMSD (Å) during an MD simulation of mGlu5 with photoexcited (*cis*-azo) alloswitch-1.